

Quarterly Technical Report

Reactive Multiphase behavior of CO₂ in Saline Aquifers beneath the Colorado Plateau

Reporting Period Start Date: October 1 2002
Reporting Period End Date: December 31 2002

Principal Authors: R. G. Allis (Utah Geological Survey)
J. Moore (Energy & Geoscience Institute)
S. White (Industrial Research Limited)

Date Report Issued January 30, 2003

DOE Award Number: DE-FC26-00NT40926

Submitted By: University of Utah, Salt Lake City UT 84108
In Collaboration With: Utah Geological Survey, PO Box 146100, Salt Lake City UT 84114
Industrial Research Ltd, PO Box 31-310, Lower Hutt, New Zealand

Disclaimer

This report was prepared as an account of work sponsored by an agency of the United States Government. Neither the United States Government nor any agency thereof, nor any of their employees, makes any warranty, express or implied, or assumes any legal liability or responsibility for the accuracy, completeness, or usefulness of any information, apparatus, product, or process disclosed, or represents that its use would not infringe on privately owned rights. Reference herein to any specific commercial product, process, or service by trade name, trademark, manufacturer, or otherwise does not necessarily constitute or imply its endorsement, recommendation, or favoring by the United States Government or any agency thereof. The views and opinions of authors expressed herein do not necessarily state or reflect those of the United States Government or any agency thereof.

ABSTRACT

Gas reservoirs developed within the Colorado Plateau and Southern Rocky Mountains region are natural laboratories for studying the factors that promote long-term storage of CO₂. They also provide sites for storing additional CO₂ if it can be separated from the flue gases of coal-fired power plants in this part of the U.S.A. These natural reservoirs are developed primarily in sandstones and dolomites; shales, mudstones and anhydrite form seals. In many fields, stacked reservoirs are present, indicating that the gas has migrated up through the section. There are also geologically young travertine deposits at the surface, and CO₂-charged groundwater and springs in the vicinity of known CO₂ occurrences. These near-surface geological and hydrological features also provide examples of the environmental effects of leakage of CO₂ from reservoirs, and justify further study.

During reporting period covered here (the first quarter of Year 3 of the project, i.e. October 1 – December 31, 2002), the main achievements were:

- Planning workshop for project participants as well as other Utah researchers involved in CO₂ projects (22 October, 2002, and Utah Geological Survey, Salt Lake City)
- Presentation of paper to special CO₂ sequestration session at the Geological Society of America Annual Meeting, Denver, 29 October, 2002
- Presentation of paper to special CO₂ sequestration session at the Fall Meeting of American Geophysical Union, San Francisco, 10 December, 2002
- Identification of dawsonite (sodium-aluminum carbonate) as a late stage mineral deposited in CO₂ feedzone at Springerville, Arizona
- Successful matching of known physical constraints to flow beneath the Hunter cross-section being used to simulate the effects of CO₂ injection. In about 1000 years, most injected CO₂ may be lost to the surface from the three shallowest reservoirs considered, assuming no reactive processes
- Inclusion of reactive processes in numerical simulations, and indication that CO₂ is sequestered for at 1000 years in form of dissolved CO₂ and carbonate mineral precipitation.

- **TABLE OF CONTENTS**

	Page
● LIST OF GRAPHS AND TABLES	4
● EXECUTIVE SUMMARY	5
● EXPERIMENTAL	6
● RESULTS AND DISCUSSION	6
● REFERENCES	13

LIST OF GRAPHS AND TABLES

	Page
Table 1: Properties of geologic units forming the cross-section in Figure 1.	15
Table 2: Capillary pressure parameters for different permeabilities.	15
Table 3: Reservoir mineralogy, the key to the references is given below.	16
Table 4: Initial Reservoir Mineralogy (%). The code for formation names is given in Table 1.	17
Figure 1: Geology on the cross-section beneath the Hunter Power-plant, Central Utah	18
Figure 2: Cross-section on which the model is based. Symbols indicate the location of pressure data points used in calibrating the model. Data points on the East San Raphael swell are to the east of the cross-section and provide a boundary condition on the Eastern boundary of the slice.	19
Figure 3: Integrated finite difference grid used in calculations. Note that the vertical scale is exaggerated by a factor of almost 50.	20
Figure 4. Mercury injection porosimetry (MIP) measurements on 10 selected seal rock core samples and five reservoir rock core samples from the Colorado Plateau.	21
Figure 5: Parameterisation of capillary pressure curves shown in Figure 3	21
Figure 6: Comparison between measurement and calculated pressure values. Note that the East San Raphael swell values lie to the East of the model cross-section and provide boundary conditions on the Eastern boundary.	22
Figure 7: Fraction of total injected CO ₂ contained within the earth as a function of time for three potential sequestration sites. Note that these calculations ignored water-rock reactions.	23
Figure 8: Gas location when injection is into the White Rim formation.	24
Figure 9: Changes in reservoir mineralogy as a result of reacting with a brine in equilibrium with CO ₂ at 260 Bars. Porosity is not included in the calculation of mineral fraction.	25
Figure 10: Change in reservoir porosity through reaction with CO ₂ rich brine.	26
Figure 11: CO ₂ sequestered as a mineral or dissolved in reservoir fluid.	27

EXECUTIVE SUMMARY

Most of the effort this quarter has concentrated on incorporating reactive processes into numerical simulation of injected CO₂, and is reviewed in this report. Significant additional work occurred on petrological and geochemical evidence for fluid-rock interactions in the reservoir of the Springerville CO₂ field in Eastern Arizona. One important finding was recognition of dawsonite, a sodium aluminum carbonate, as a late-stage alteration mineral in a major CO₂ feedzone at Springerville. The occurrence of this carbonate mineral had been suspected in clastic CO₂ reservoirs, but had never been reported in the U.S.

Two examples of technical transfer for this project occurred during the reporting period. Both were at national conferences that had special sessions on CO₂ sequestration. One was the Geological Society of America annual meeting (October, 2002, Denver), and the other was the American Geophysical Union fall meeting (December, 2002, San Francisco). The two papers reviewed progress on this project, and gave opportunities for further discussions with other researchers working in this area.

Numerical modeling included natural state matching of known physical constraints to flow beneath the Hunter cross-section in central Utah, which is adjacent to two large coal-fired power plants. Once the natural state conditions were satisfactorily matched, the effects of CO₂ injection were simulated, initially assuming non-reactive processes, and then with fluid-rock interactions included. In about 1000 years, most injected CO₂ may be lost to the surface from the three shallowest reservoirs considered, assuming no reactive processes. Inclusion of reactive processes indicates that CO₂ is sequestered for at 1000 years in form of dissolved CO₂ and carbonate mineral precipitation. These preliminary results suggest that this site may be suitable for sequestration of flue gas CO₂.

EXPERIMENTAL

Not applicable

RESULTS AND DISCUSSION

This quarter, most of the effort concentrated on incorporating reactive processes into numerical simulation of injected CO₂. Most of this report reviews modeling progress. Significant additional work occurred on petrological and geochemical evidence for fluid-rock interactions in the reservoir of the Springerville CO₂ field in Eastern Arizona. One important finding was recognition of dawsonite, a sodium aluminum carbonate, as a late-stage alteration mineral in a major CO₂ feedzone at Springerville. The occurrence of this carbonate mineral had been suspected in clastic CO₂ reservoirs, but had never been reported in the U.S. This work will be documented during the first quarter of 2003, and results will be summarized in the next quarterly report.

Two major technical transfer contributions occurred during the reporting period. Rick Allis presented a paper on aspects of this project to the Annual Meeting of the Geological Society of America in Denver, on October 29, 2002. This paper was part of two special sessions addressing geological sequestration of CO₂. The title, authors and abstract were:

CO₂ geysers, springs and massive travertine deposits in central Utah and eastern Arizona: examples of natural leakage of fluids saturated in CO₂.

R.G. Allis¹, J. N. Moore², T. Chidsey¹, C. Morgan¹, W. Gwynn¹, H. Doelling¹, M. Adams², S. Rauzi³, S. White⁴

¹ Utah Geological Survey, Salt Lake City, Utah

² Energy and Geoscience Institute, University of Utah, Salt Lake City

³ Arizona Geological Survey, Tucson, Arizona

⁴ Industrial Research Ltd, Lower Hutt, New Zealand

Abstract

Extensive travertine deposits occur over 50 - 100 square mile areas near the Green River in central Utah, and the Little Colorado River between Springerville and St. Johns in eastern Arizona. Both areas occur adjacent to fault zones with significant differential vertical displacement of Colorado Plateau strata. Analysis of drill stem pressure measurements from deep exploration wells, and potentiometric data from groundwater, springs and CO₂ geysers, suggests that these areas are outflow zones of deep basin fluids saturated in CO₂ originating from aquifers up to 1000 square miles in area. Older travertine caps terraces and forms domes that are up to 200 feet above the presently active seepage areas. Based on erosion rate estimates of less than one foot per thousand years for the Colorado River system in Utah, the fluid outflow has been active for at least several hundred thousand years. These areas may be natural analogues for some of the potential effects of CO₂ leakage from subsurface reservoirs with imperfect seals.

•

The second paper was presented to a special session at the Fall Meeting of the American Geophysical Union with the theme “Carbon Sinks and Carbon Management: Scientific Perspectives on Potential Benefits and Consequences” (December 10, 2002, San Francisco). Details of the paper are:

Geological Storage of CO₂ Beneath the Southern Rocky Mountains-Colorado Plateau Region

Rick Allis¹ and Steve White²

¹ Utah Geological Survey, Salt Lake City, Utah

² Industrial Research Ltd., Lower Hutt, New Zealand

Abstract

The Southern Rocky Mountains-Colorado Plateau region presents unusual scientific opportunities for studying the effects of geological storage of CO₂. An abundance of oil and natural gas fields, as well as natural CO₂ fields, proves the existence of reservoirs and seals in the sediments that are suitable for long-term gas storage. The widespread occurrence of near-surface coal measures has resulted in large coal-fired power plants being collocated in the same region. The six largest power plant sites are point sources of 100 million tonnes/year of CO₂, and four natural CO₂ fields produce over 30 million tonnes/year mostly for enhanced oil recovery. Structures near to these power plants, as well as the produced natural CO₂ fields could provide storage for significant volumes of CO₂ separated from power plant flue gases.

We report on the latest findings from a multi-disciplinary study using the natural CO₂ fields as analogues for long term CO₂ storage. The frequent presence of stacked reservoirs in these systems and obvious outflow of CO₂-rich fluids in the vicinity of two known CO₂ areas suggests that it is unrealistic to expect total containment of CO₂. Local containment in a domal or stratigraphic trap may also not be a requirement for long-term storage. Dipping or undulating reservoir structures that are not laterally confined may actually be preferable because of the opportunity for long flow paths and a long time scale that promotes permanent sequestration of injected CO₂, either as a mineral or dissolved in groundwater. Results of two-dimensional, two-phase reactive transport modeling of CO₂ injection into a dipping sedimentary sequence beneath a large power plant in central Utah will be presented.

The remainder of this report is concerned with the progress of the numerical simulation task.

Numerical Simulation Task

Work this quarter has concentrated on the injection of CO₂ into geological structures that are not dome shaped and thus do not provide the geometry required for the development of an artificial CO₂ reservoir. Such structures may, however, provide very long flow paths between the injection point and the surface, allowing the permanent sequestration of injected CO₂ as a mineral or dissolved in the groundwater.

The geology beneath Hunter Power Plant, located in central Utah, is one example of such a structure. This geology is shown in Figure 1 and the location of the cross-section in Figure 2. The sedimentary sequence shown in Figure 1 contains potential reservoir and seal formations at over 1 km depth beneath the power plant, but the regional dip exposes some of these formations at the surface some 40 - 50 km away.

Table 1 summarizes the properties of the units in the sequence and identifies several potential targets for the injection of CO₂ gas on this cross-section

- Navajo Sandstone
- Wingate Sandstone,
- White Rim Sandstone,
- Redwall Limestone.

Of these, only the Redwall Limestone is not exposed on the crest or flanks of the uplift.

Significant amounts of CO₂ have been found in the Sinbad Limestone, a member of the Moenkopi formation, at the Gordon Creek field located to the northwest of the uplift. This formation is not considered a candidate for injection because it is relatively thin, 50 to 150 feet (15-46 m), with low permeability and porosity. What permeability and porosity are present in the Sinbad Limestone, are the result of fracturing.

Navajo Sandstone

The eolian Jurassic Navajo Sandstone is one of the best candidates for CO₂ injection, because it generally has excellent porosity and permeability. It has produced CO₂ at Farnham Dome on the north plunging nose of the San Rafael uplift. The Navajo is 450 to 600 feet (137-183 m) thick in the uplift and relatively homogeneous. However, it is exposed and deeply incised along both the gently dipping west flank and steeply dipping east flank of the uplift. The Navajo would best be targeted in subsidiary structures along the west flank of the uplift. On these structures, shale and anhydrite beds would effectively seal the Navajo in the overlying 240 to 300-foot-thick (73-91 m) Jurassic Carmel Formation. Flow paths would likely be along major fracture or joint systems, and minor high angle normal faults present in the region.

Wingate Sandstone

The eolian Jurassic Wingate Sandstone is a CO₂ injection candidate similar to the Navajo Sandstone. Although little petrophysical work is available, it is likely that it has good porosity and permeability. The Wingate is 300 to 400 feet (91-122 m) thick in the uplift and relatively homogeneous. But like the Navajo, the Wingate is also exposed and deeply incised along the flanks of the San Rafael uplift. Therefore, the Wingate too would best be targeted in subsidiary structures along the west flank of the uplift. Where the Wingate outcrops, it typically displays closely spaced vertical joints. Any injected CO₂ would likely migrate along these joints and into and through the overlying Kayenta Formation, a 50 to 300-foot-thick (15-91 m), heterogeneous fluvial deposit consisting of interbedded sandstone, siltstone, and shale. Ultimately the gas would migrate and accumulate in the Navajo above the Kayenta.

White Rim Sandstone

The eolian Permian White Rim Sandstone is the best candidate for CO₂ injection. It has excellent porosity and permeability. It is the main CO₂ reservoir at the Gordon Creek field. The White Rim is 200 to 800 feet (61-244 m) thick in the uplift and relatively homogeneous. The upper White Rim is oldest formation exposed on the San Rafael uplift. The White Rim crops out along the asymmetrical crest of the uplift and in a few of the canyons on the east flank. The White Rim would be effectively sealed by tidal flat shale and mudstone beds in the overlying 490 to 1050-foot-thick (149-320 m) Triassic Moenkopi Formation. The White Rim and Moenkopi are separated by the Permian Black Box Dolomite ranging in thickness from 0 to 200 feet (0-61 m). Flow paths would likely be along major fracture or joint systems, and minor high angle normal faults present in the region.

Redwall Limestone

The shallow marine Mississippian Redwall Limestone is the deepest candidate for CO₂ injection and is not exposed in the San Rafael uplift. It has moderate porosity and permeability, and is a major producer of oil and gas in structural traps (faulted anticlines) to the southeast in the Paradox Basin. Testing has shown significant flow rates of CO₂ from several wells in the basin although never been produced commercially. The Redwall is 600 to 1,000 feet (183-305 m) thick in the San Rafael uplift but likely has a fair amount of heterogeneity due to changes in depositional facies and carbonate diagenetic effects. The Redwall would be effectively sealed by marine shale of the overlying 100 to 500-foot-thick (30-152 m) Pinkerton Trail Formation and marine shale and anhydrite of the 300 to 1,000-foot-thick (91-305 m) Paradox Formation, both Pennsylvanian in age. Flow from the Redwall beyond the Pinkerton and Paradox seals would be along high angle normal faults that may be present in the subsurface.

Hydrological model

The regional topography and precipitation pattern give a pressure gradient roughly along the cross-section of Figure 1, with pressures highest in the West. Regional flow is from the high ground of the Wasach Plateau in the West towards the Green River in the East.

1. Precipitation and Recharge

In the Wasach Plateau region (topography above roughly 2000 m asl) annual precipitation ranges from 100 cm at the West of the section to 20 cm where the surface drops below 2000 m asl. East of this the annual precipitation is 20 cm. Infiltration is taken to be 15% on the High Plateau, above 2500 masl and 2% elsewhere. These values are similar to those assumed by USGS hydrologic modeling of the Colorado Plateau, and one particular study of recharge amounts not too far from the cross-section of Figure 1 (Danielson and Hood, 1984).

2. Porosity and permeability properties

Earlier work under this project modeled the formation of the natural CO₂ reservoirs at Farnham Dome on the Colorado Plateau (Allis *et. al* 2001, White *et. al* 2001, White *et. al* 2002). This work found that permeabilities of 100 mD for aquifers, 1 mD for mixed units, and 0.01 mD for confining units lead to the formation of the observed natural CO₂ reservoirs. Increasing these figures by an order of magnitude did not give rise to the formation of reservoirs.

We have reviewed several USGS hydrologic studies on the Colorado Plateau and their estimates of hydraulic conductivities are consistent with the values found in the Farnham Dome modeling. Freethey and Cordy, (1991) is a particularly good review of the Mesozoic unit hydrologic properties of this region. This paper assembles hydraulic conductivity ranges for “aquifers” and “confining units”, using data from lab tests, drill stem tests, specific capacity tests, and aquifer tests. The aquifer tests show conductivities ranging between about 0.1 and 50 ft/day, so taking 1 - 2 ft/day as the mode, implies a permeability of 0.3 – 0.6 mD for aquifers.

The fact that conductivity data for both aquifers and aquicludes overlap significantly and has such a range highlights the natural variability of the units, and the problem of measuring permeabilities on different scales, from centimeters in the lab to hundreds of meters regionally.

For the current work permeabilities were initially set to the values used for the Farnham Dome modeling (100 mD for aquifers, 1 mD for mixed units, and 0.01 mD for confining units) and these values refined to match the observed pressure distribution on the cross-section.

3. Lateral Flow

We believe most recharge gets split between short range discharge in and adjacent to the steep terrain adjacent to the Plateau, and a component that goes deep, eventually discharging in the vicinity of the Green River.

Hydrologic studies in the Green River discharge area to the east suggest a groundwater inflow of 20 l/s per km of river length (Rush et al., 1982). Probably, the bulk of this comes from the west and northwest, but to be conservative, we assume half of this comes from the west (i.e. direction of our cross-section = 10 l/s). Since there is negligible discharge between the San Rafael Swell and the Green River, this figure provides a constraint on the lateral flow across the eastern boundary of the modeled section.

On the eastern boundary of the model we set boundary pressures to those of a hydrostatic column with the water table depth determined from pressure measurements in the area.

Numerical Model

A TOUGH2 integrated finite difference model of the cross-section shown in Figure 1 has been developed. The area has been divided into a number of elements with element geometry determined by the need to match geological layer interfaces and the need for a fine grid in the vicinity of the injection wells. This grid is shown in Figure 3.

Boundary Conditions

Boundary conditions for the numerical model are determined largely from the hydrological model discussed earlier and they can be summarized as

- Atmospheric pressure at the surface
- 20 cm precipitation on low area with 2% infiltration
- 100 cm precipitation in the West decreasing to 20 cm at the base of the Wasatch Plateau with 15% infiltration
- Constant pressure on the Eastern boundary
- Constant pressure on Western boundary during injection
- No fluid flow at base
- Heat flow at base to match normal terrestrial flow

Parameters

Capillary pressure functions

The presence of rocks capable of withholding a significant thickness of injected CO₂ is a critical aspect of any potential CO₂ sequestration site. We reported on mercury injection porosimetry (MIP) to quantify the sealing characteristics of major, low permeability formations on the Colorado Plateau in the October – December 2001 quarterly report of this project. Figure 4 is taken from this report and summarizes the results of the MIP measurements.

There are a number of analytic descriptions of capillary pressure curves available in the literature (e.g. Pickens et al. 1979, Leverett 1941, van Genuchten 1980) but none of these reproduced the measured curves to an acceptable degree. Therefore we parameterized the measured curves using five parameters as shown in Figure 5.

Capillary pressure functions were assigned to the three permeabilities using the parameters given in Table 2.

Permeability

Initially permeability values of 100 mD for aquifers, 1 mD for mixed units, and 0.01 mD for confining units were assigned and a steady state calculated using the boundary conditions described above. These values provided an acceptable match to measured steady state pressures but it was found that this match was improved, particularly in the Wasach Plateau region, by using higher permeabilities. The final values arrived at were 200 mD for aquifers, 2 mD for mixed units, and 0.02 mD for confining units and Figure 6 shows the match between model values and measurement.

Changing the permeability values raised the concern that the new values might not be compatible with the formation of the natural CO₂ reservoirs at the nearby Farnham Dome field. Rerunning

the Farnham Dome simulation showed that natural CO₂ reservoirs were indeed formed using these new estimates of permeability.

Sequestration scenarios

We investigated injection into the Navajo sandstone, White Rim sandstone, Wingate sandstone and Redwall Limestone aquifers. Results are not presented for the Redwall Limestone as this reservoir proved unsuitable for long-term sequestration. Very high injection pressures were required to inject into this intermediate permeability reservoir. In all cases reported CO₂ is injected for 30 years at 0.15 kg/s per meter of cross-section thickness, this rate corresponds to about 5 Mtonne / year (approximately equal to the emissions from a 600 MW coal fired power station) into a section 100 meters thick.

In the initial simulations reaction between the CO₂ rich brine and the reservoir rocks was ignored. These reactions were included in later modeling of the most promising site for sequestration, the White Rim sandstone.

Figure 7 shows the fraction of injected CO₂ that has not returned to the atmosphere as a function of time. Water-rock reactions have been ignored in the calculation of these results. Clearly neither the Wingate nor Navajo formations appear suitable for long-term sequestration of CO₂. In both formations CO₂ begins to reach the surface before injection completes. The location of the injected CO₂ when injection is into the White Rim sandstone is shown in Figure 8. Even in this case there is significant leakage from the target reservoir and a much larger volume of rock is exposed to CO₂ than just the White Rim sandstone formation.

In order to establish a timescale for significant mineral sequestration of CO₂ we modeled the reactions between reservoir brine in equilibrium with CO₂ at 260 bars and simplified reservoir mineralogy over a period of 100,000 years. Reservoir temperature was set to 54°C for these calculations. The major changes in reservoir minerals are shown in Figure 9. Initially Anorthite is dissolved and the calcium from this reaction is precipitated as calcite. This is followed by the dissolution of Albite accompanied by the precipitation of Kaolinite and finally the slow dissolution of K-feldspar. There is little change after 1000 years. These reactions are accompanied by an increase in fluid pH as dissolution of the feldspars partially neutralizes the initially acid fluid. A small decrease in porosity accompanies these reactions but overall the change is not sufficient to reduce the permeability significantly.

Figure 10 gives a timescale for mineral sequestration, the mineral sequestration reactions are largely complete by 100 years at which stage about 100 moles CO₂ are sequestered as a mineral per cubic meter of rock (about 4 kg/m³).

The capacity of White Rim sandstone for sequestration (assuming a 100 meter wide cross-section) is approximately $50,000 \times 100 \times 200 \times 4.4 = 4.4 \times 10^9$ kg or sufficient to sequester about 30 years of injected CO₂. CO₂ is sequestered as a mineral or dissolved in reservoir fluid. In fact, a much larger volume of rock is 'seen' by the injected CO₂ than is contained in the White Rim formation (see Figure 8) and there should be ample volume of rock to sequester all the injected CO₂ providing flow to the surface is sufficiently slow.

Only the White Rim formation provides containment of injected CO₂ for the hundreds of years required for mineral sequestration reactions to complete. However, the geochemical situation is much more complex than has been modeled so far. Transport of reaction products in the reservoir, changing reservoir temperature, mineralogy and partial pressure of CO₂ all mean a full reactive transport model must be used.

Reactive transport model

Reactive transport modeling is a computer intensive activity and a balance must be struck between model complexity and resolution and computer time. We have included sufficient geochemical complexity to represent the interaction of the observed reservoir mineralogy with CO₂ rich brine. To achieve this the spatial resolution of the model has been reduced and the grid does not contain the fine resolution about the injection point shown in Figure 3. However it retains a reasonable resolution with over 1300 elements.

Initial chemical conditions were calculated by firstly assigning the mineralogy specified in Table 4 to model elements, setting the reservoir fluid to a 0.3 M NaCl brine and then allowing the brine to react with the reservoir for 150 years. This provided an initial mineralogy and fluid reservoir throughout the reservoir. CO₂ was then injected into the White Rim formation for 30 years at the same rate as used in the non-reactive modeling described earlier in this report. The chemistry and flows in the system were then simulated for a total of 1000 years.

REFERENCES

- Allis, R., White, S., Chidsey, T, Gwynn, W., Morgan, C. Adams, M., Moore, J., 2001. Natural CO₂ Reservoirs on the Colorado Plateau and Southern Rocky Mountains: Candidates for CO₂ Sequestration, *Proceedings of the First National Conference on Carbon Sequestration*, Washington DC, May 2001.
- Blum, A. E., and Stillings, L. L., 1995, Feldspar dissolution kinetics, Chapter 7 of chemical weathering rates of silicate minerals, White, A.F., and Brantley, S. L. (Eds.), *Mineral Society of America*, v. 31, p. 291–351, Washington D. C.
- Danielson, T.W. and Hood, J.W., 1984. Infiltration to the Navaho sandstone in the Lower Dirty Devil River Basin, Utah, with emphasis on techniques used in its determination. *U.S. Geol. Surv. Water Investigations Report 84-4154*, pp. 45.
- Freethy, G.W. and Cordy, G. 1991. Geohydrology of Mesozoic rocks in the Upper Colorado River Basin in Arizona, Colorado, New Mexico, Utah, and Wyoming, excluding the San Juan Basin. *U.S. Geol. Surv. Prof. Paper 11411-C*, pp. 118.
- Knauss, K. G., and Wolery, T. J., 1989, Muscovite dissolution kinetics as a function of pH and time at 70°C.” *Geochimica et Cosmochimica Acta*, v. 53, p. 1493–1501.
- Leverett, M.C. Capillary Behavior in porous solids, *AIME Trans*, Vol 142, p152, 1941

Nagy, K. L., Dissolution and precipitation kinetics of sheet silicates, 1995, *Chemical Weathering Rates of Silicate Minerals*, v. 31, p. 291–351.

Oelkers, E.H. and Schott, J, 1995, experimental study of anorthite dissolution and the relative mechanism of feldspar hydrolysis. *Geochimica et Cosmochimica Acta*, v. 59, p. 5039–5053.

Pickens, J.F., Gillham, R.W. and Cameron, D.R. Finite Element Analysis of the Transport of water and Solutes in Tile-Drained Soils. *J. of Hydrology*, 40, pp 243-264 1979

Rush, F.E., Whitfield, M.S., and Hart, I.M. 1982. Regional hydrology of the Green River-Moab area, Northwestern Paradox basin, Utah. *U.S. Geol Surv. Open-File Report 82-107*, pp. 86, Denver, CO.

Svensson, U. and Dreybrodt, W., 1992. Dissolution kinetics of natural calcite minerals in CO₂-water systems approaching calcite equilibrium.” *Chemical Geology*, v. 100, p. 129–145. Amsterdam, The Netherlands, Elsevier Science Publishers.

Tester, J. W., Worley, G. W., Robinson, B. A., Grigsby, C. O., and Feerer, J. L., 1994, Correlating quartz dissolution kinetics in pure water from 25° to 625 °C., *Geochimica et Cosmochimica Acta*, v. 58, p. 2407–2420.

Van Genuchten, M. T., A Closed-Form equation for Predicting the hydraulic Conductivity of Unsaturated Soils, *Soil Sci. Soc. Am. J. Vol. 44* pp 892-898 ,1980

White, S., Weir, G. and Kissling, W., 2001 Numerical Simulation of CO₂ Sequestration in Natural CO₂ Reservoirs on the Colorado Plateau, *Proceedings of the First National Conference on Carbon Sequestration*, Washington DC, May 2001.

White, S., Allis, R., Moore, J., Chidsey, T., Morgan, C., Gwynn, W., Adams, M., 2002 Natural CO₂ Reservoirs on the Colorado Plateau and Southern Rocky Mountains, USA, A Numerical Model. *Proceedings Sixth International Conference on Greenhouse gas control Technologies Kyoto 2002* (to be published).

Formation	Typical Thickness (meters)	Age	Porosity	Permeability	Potential as a CO ₂ Reservoir	Potential as a Seal
North Horn Tkn	<250	Tertiary	High	Med	Too shallow	
Price River Kpr	80	Cretaceous	High	Med	Too shallow	
Castlegate Kc	70	Cretaceous	High	High	Too shallow	
Blackhawk Kbh	120	Cretaceous	Med	High	Too shallow	
Star Point Ksp	60	Cretaceous	Med	Med	Too shallow	
Mancos Kmm	380	Cretaceous	Low	Low	Low	Med
Mancos Kmem	120	Cretaceous	Med	Med	Low	Med
Mancos Kmbg	200	Cretaceous	Low	Low	Low	High
Mancos Kmf	10	Cretaceous	High	High	Low	High
Mancos Kmt	20	Cretaceous	Low	Low	Low	High
Dakota and Cedar Mtn. Undivided Kdc	87	Cretaceous-Jurassic	Med	Med	Med	Low
Morrison Jms	201	Jurassic	Med	Med	Med	Low
Summerville/Curtis Js	82	Jurassic	Low	Low	Low	High
Entrada Je	136	Jurassic	Med	Low	Low	Low
Carmel Jc	82	Jurassic	Low	Low	Low	Med
Navajo Jn	160	Jurassic	High	High	High	Low
Kayenta Jk	53	Jurassic	Med	Med	Low	Low
Wingate Jw	107	Jurassic	High	High	High	Low
Chinle Trc	113	Triassic	Low	Low	Low	High
Moenkopi Trm	235	Triassic	Low	Low	Low	High
Black Box Pk	31	Permian	Med	Low	Low	Med
White Rim Pwr	153	Permian	High	High	High	Low
Elephant Canyon Pec	198	Permian	Low	Low	Low	Med
Honaker Trail Pht	190	Pennsylvania n	Med	Low	Low	Low
Paradox Pp	198	Pennsylvania n	Med	Low	Low	High
Pinkerton Trail Ppt	91	Pennsylvania n	Low	Low	Low	Med
Redwall Mr	244	Mississippian	Med	Med	Med	Low
Ouray Do	53	Devonian	Low	Low	Low	Med
Elbert De	76	Devonian	Low	Low	Low	Med
Lynch-Maxfield undivided Clm	312	Cambrian	Low	Low	Low	Med
Ophir Co	61	Cambrian	Low	Low	Low	High
Tintic Ct	62	Cambrian	Low	Low	Low	Low
Schist/Granite Pc	--	Precambrian	Low	Low	Low	Low

Table 1: Properties of geologic units forming the cross-section in Figure 1.

Permeability	P0	P1	P2	S1	S2
Low	3.92×10^7	1.20×10^7	6.66×10^3	0.60	0.95
Medium	3.92×10^7	6.60×10^5	6.60×10^3	0.70	1.0
High	3.92×10^7	1.10×10^5	3.90×10^3	0.05	1.0

Table 2: Capillary pressure parameters for different permeabilities.

Mineral	Chemical composition	Volume (%)	Surface area (m ² /dm ³ medium)	k ₂₅ (moles m ⁻² s ⁻¹)	E _a (KJ/mol)	Ref.
Quartz	SiO ₂	77	7.7	1.2589x10 ⁻¹⁴	87.5	1
K-feldspar	KAlSi ₃ O ₈	0.60	0.060	1.00x10 ⁻¹²	67.83	2
Kaolinite	Al ₂ Si ₂ O ₅ (OH) ₄	2.25	22.5	1.00x10 ⁻¹³	62.76	3
Calcite	CaCO ₃	1.80	0.180	1.60x10 ⁻⁹	41.87	4
Dolomite	CaMg(CO ₃) ₂	0.0	25.0	0.60x10 ⁻⁹	41.87	5
Siderite	FeCO ₃	0.0	25.0	0.60x10 ⁻⁹	41.87	5
Illite	K _{0.6} Mg _{0.25} Al _{1.8} (Al _{0.5} Si _{3.5} O ₁₀)(OH) ₂	0.0	25.0	1.00x10 ⁻¹⁴	58.62	6
Glauconite	K _{1.5} Mg _{0.5} Fe _{2.5} Fe _{0.5} AlSi _{7.5} O ₂₀ (OH) ₄	0.0	25.0	1.00x10 ⁻¹⁴	58.62	7
Albite-low	NaAlSi ₃ O ₈	0.60	0.060	1.00x10 ⁻¹²	67.83	2
Smectite-Na	Na _{0.290} Mg _{0.26} Al _{1.77} Si _{3.97} O ₁₀ (OH) ₂	2.25	22.5	1.00x10 ⁻¹⁴	58.62	7
Anorthite	CaAl ₂ Si ₂ O ₈	0.66	0.06	1.60x10 ⁻¹⁴	18.40	8
Porosity		15.0				
Dawsonite	NaAlCO ₃ (OH) ₂	0.0	25.0	1.60x10 ⁻⁹	41.87	

Table 3: Reservoir mineralogy, the key to the references is given below.

1. Tester et al (1994)
2. Blum and Stillings (1995)
3. Nagy (1995)
4. Svensson and Dreybrodt (1992)
5. Based on Calcite
6. Knauss and Wolery (1989)
7. Based on Illite
8. Oelkers and Schott (1995)

Formation	Anorthite	Na-Smectite	Calcite	Dolomite	K-Feldspar	Kaolinite	Quartz	Gypsum	Illite	Hematite	Magnetite	Albite	Dawsonite	Siderite	Porosity
Tkn		34.	1.	1.		34.	18.		1.						10.
Tkn	1.	11.	2.		1.	11.	63.		1.			1.			10.
Kpr	1.	11.	2.		1.	11.	63.		1.	0.	0.	1.		0.	10.
Kc	1.	11.	2.		1.	11.	67.		1.	0.	0.	1.	0.	0.	5.
Kbh	1.	11.	2.		1.	11.	63.		1.	0.	0.	1.	0.	0.	10.
Ksp	1.	11.	2.		1.	11.	67.		1.	0.	0.	1.	0.	0.	5.
Kmm		37.	1.	1.		37.	20.		1.	0.	0.	0.	0.	0.	2.
Kmeu	1.	12.	2.		1.	12.	69.		1.	0.	0.	1.	0.	0.	2.
Kmem	0.	6.	1.			6.	35.		0.	0.	0.	0.	0.	0.	5.
Kmel	0.	4.	1.			4.	23.		0.	0.	0.	0.	0.	0.	2.
Kmbg	1.	12.	2.		1.	12.	69.		1.	0.	0.	1.	0.	0.	2.
Kmf		15.	2.	1.		15.	61.		1.	1.	1.	0.	0.	0.	2.
Kdc		29.	1.	1.		29.	29.		1.	0.	0.	0.	0.	0.	10.
Jmbb	1.	11.	2.	1.	1.	11.	68.		0.	1.	1.	1.	0.	0.	2.
Jms		13.	2.	1.		13.	65.		1.	1.	1.	0.	0.	0.	2.
Js	1.	11.	2.	1.	1.	11.	68.	1.	0.	0.	0.	1.	0.	0.	2.
Je	1.	5.	1.	1.	1.	5.	75.		0.	1.	1.	1.	0.	0.	10.
Jc	1.	10.	1.	52.	1.	10.	21.		1.	0.	0.	1.	0.	0.	2.
Jn	1.	2.	1.	1.	1.	2.	73.		0.	1.	1.	1.	0.	0.	20.
Jk	1.	8.	1.		1.	8.	65.		0.	0.	0.	1.	0.	0.	20.
Jw	1.	8.	1.		1.	8.	65.		0.	0.	0.	1.	0.	0.	20.
Trc	1.	22.	2.	2.	1.	22.	44.		1.	1.	1.	1.	0.	0.	2.
Trm	1.	22.	2.	5.	1.	22.	43.		0.	2.	0.	1.	0.	0.	2.
Pk		2.	2.	65.		2.	19.		0.	0.	0.	0.	0.	0.	10.
Pwr	1.	2.	2.		1.	2.	75.		0.	0.	0.	1.	0.	0.	20.
Pec				59.			39.		0.	0.	0.	0.	0.	0.	2.
Pht				28.		16.	47.		0.	2.	0.	0.	0.	0.	10.
Pp		9.		27.		9.	45.		0.	0.	0.	0.	0.	0.	10.
Ppt		37.	1.	1.		37.	20.		1.	0.	0.	0.	0.	0.	2.
Mr				90.					0.	0.	0.	0.	0.	0.	10.
Do				98.					0.	0.	0.	0.	0.	0.	2.
De		20.		59.		20.			0.	0.	0.	0.	0.	0.	2.
Clm		20.		59.		20.			0.	0.	0.	0.	0.	0.	2.
Co		20.		59.		20.			0.	0.	0.	0.	0.	0.	2.
Ct							98.		0.	0.	0.	0.	0.	0.	2.

Table 4: Initial Reservoir Mineralogy (%). The code for formation names is given in Table 1.

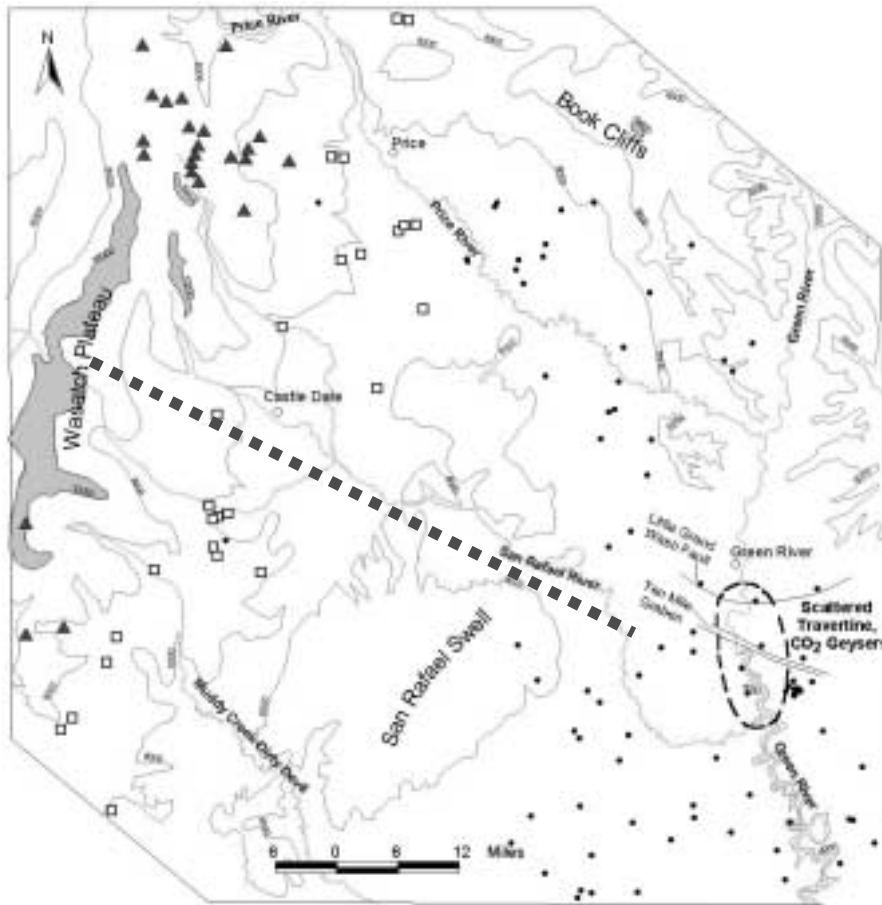


Figure 2: Cross-section on which the model is based. Symbols indicate the location of pressure data points used in calibrating the model. Data points on the East San Raphael swell are to the east of the cross-section and provide a boundary condition on the Eastern boundary of the slice.

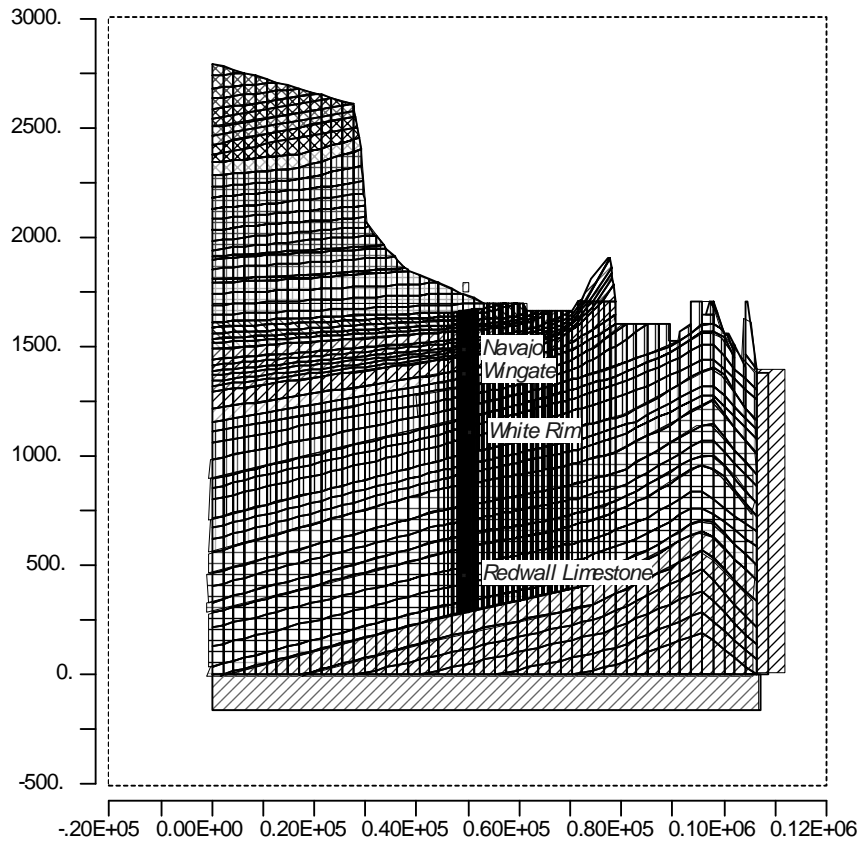


Figure 3: Integrated finite difference grid used in calculations. Note that the vertical scale is exaggerated by a factor of almost 50.

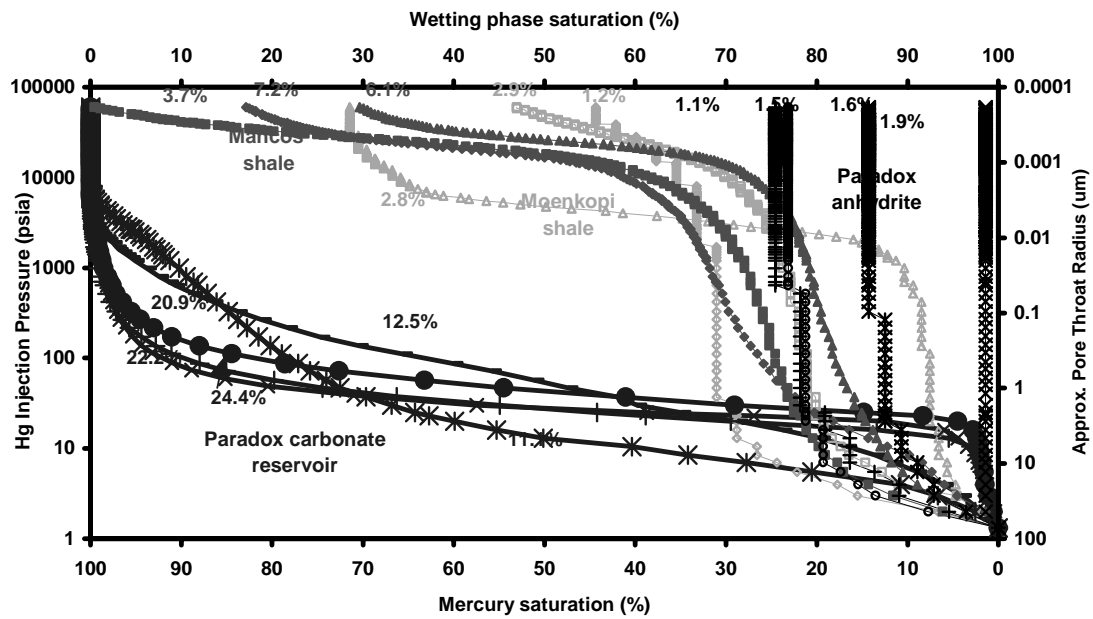


Figure 4. Mercury injection porosimetry (MIP) measurements on 10 selected seal rock core samples and five reservoir rock core samples from the Colorado Plateau.

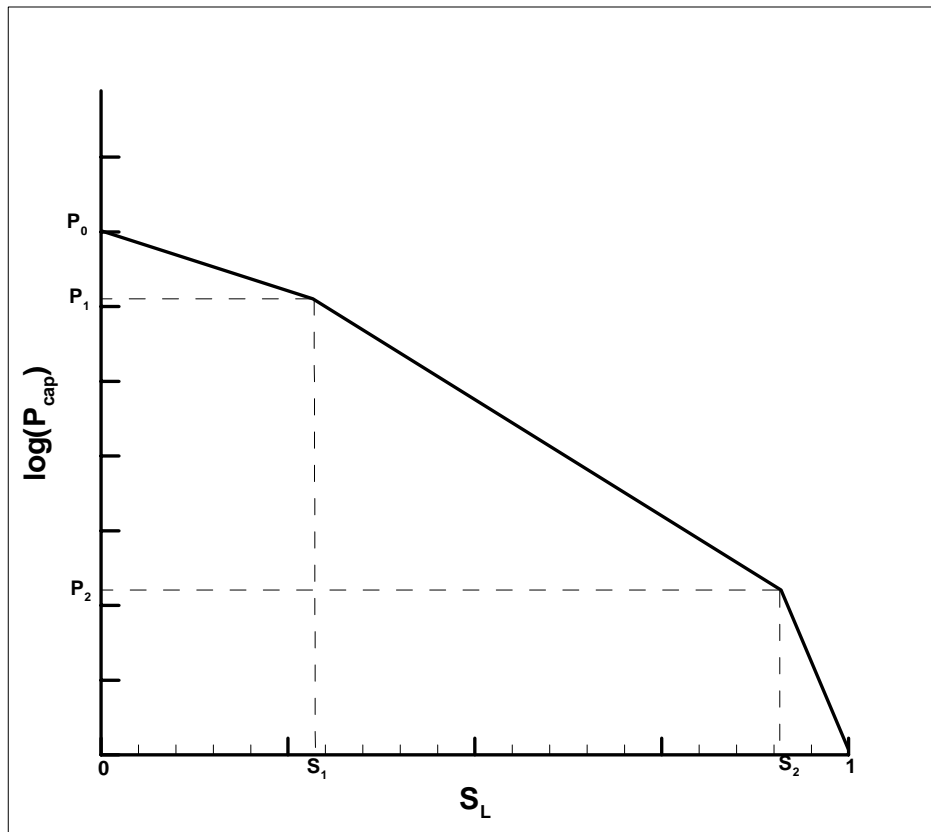


Figure 5: Parameterisation of capillary pressure curves shown in Figure 3

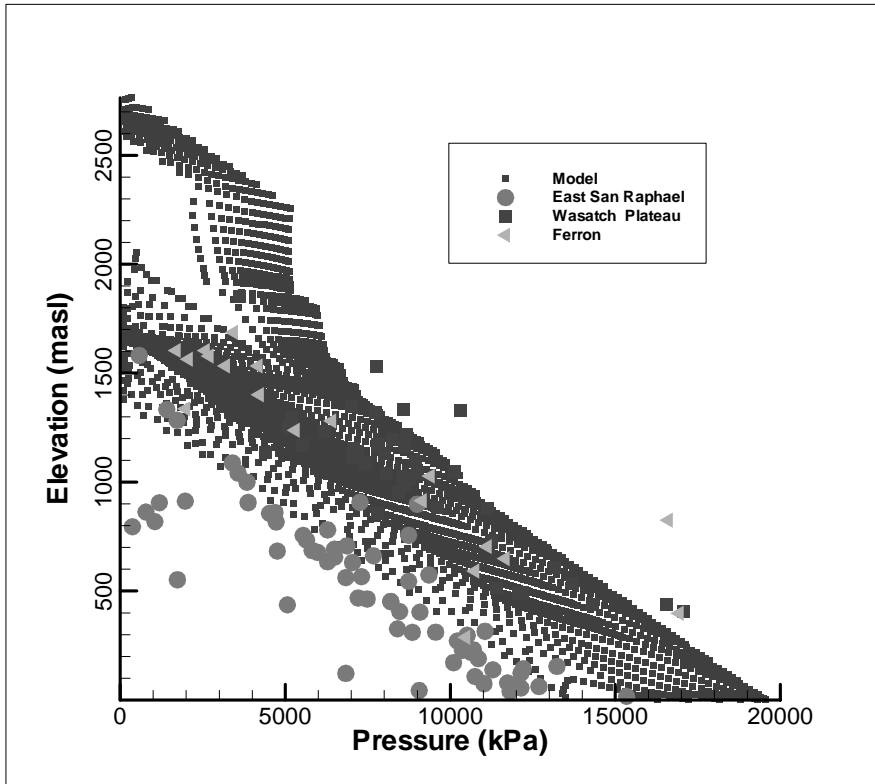


Figure 6: Comparison between measurement and calculated pressure values. Note that the East San Raphael swell values lie to the East of the model cross-section and provide boundary conditions on the Eastern boundary.

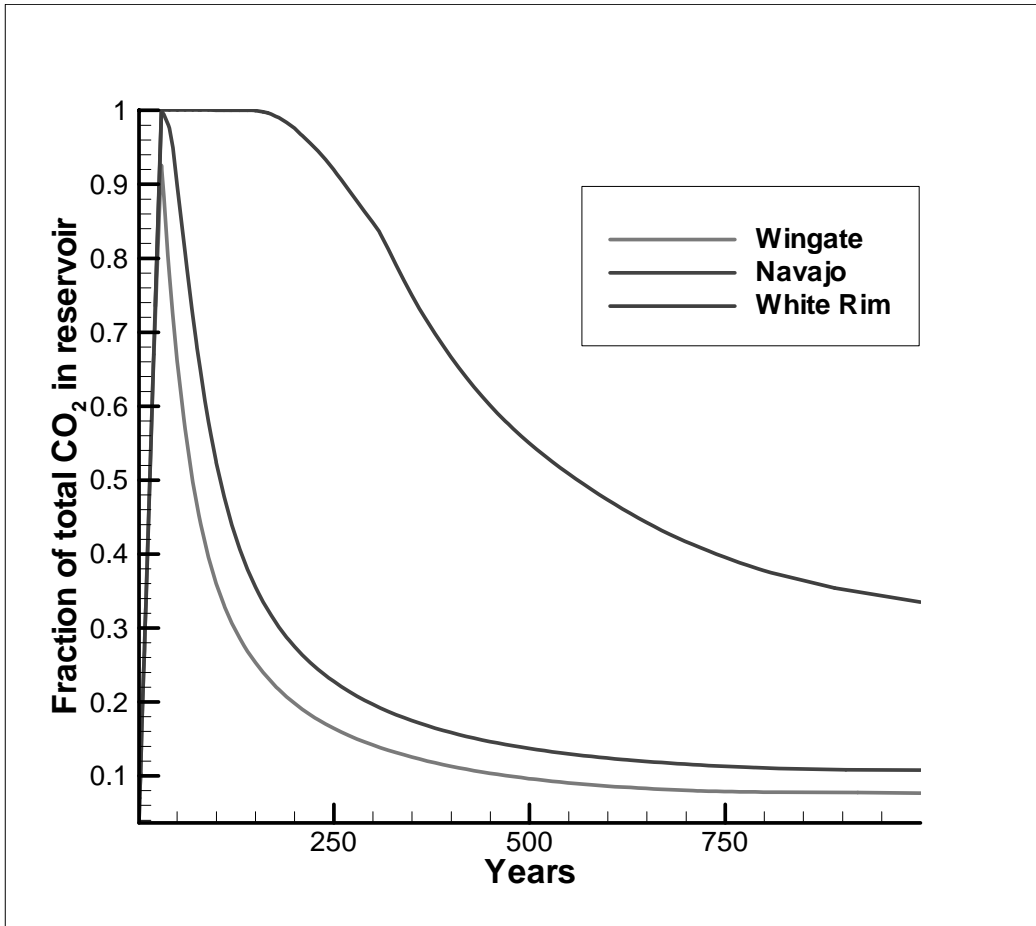


Figure 7: Fraction of total injected CO₂ contained within the earth as a function of time for three potential sequestration sites. Note that these calculations ignored water-rock reactions.

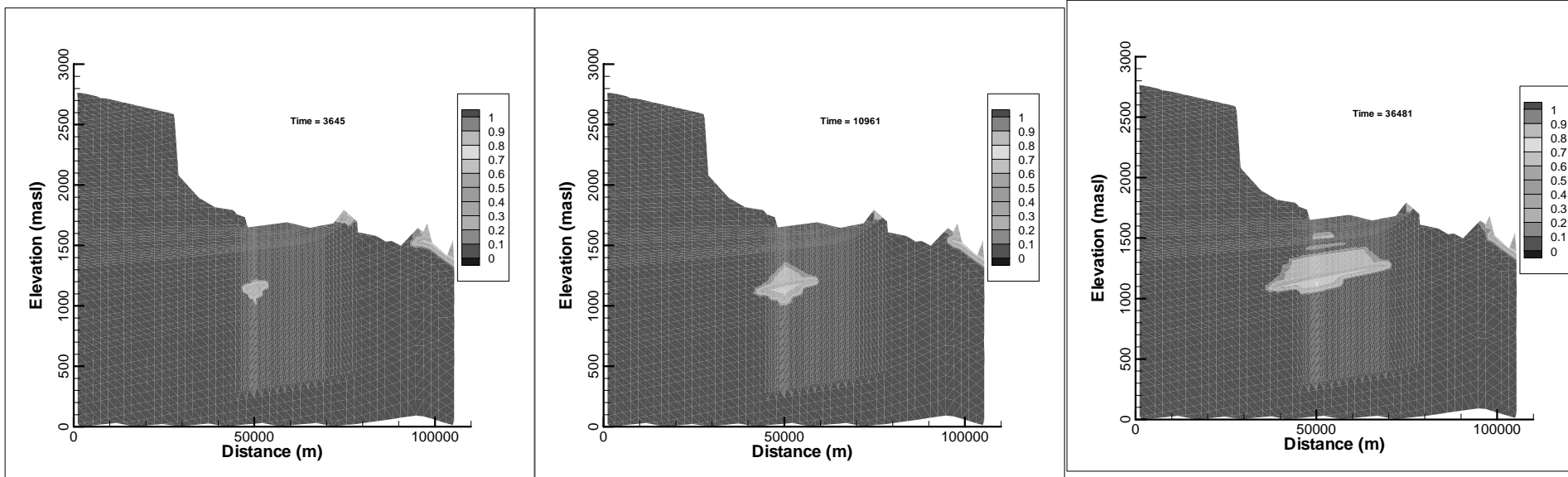


Figure 8: Gas location when injection is into the White Rim formation.

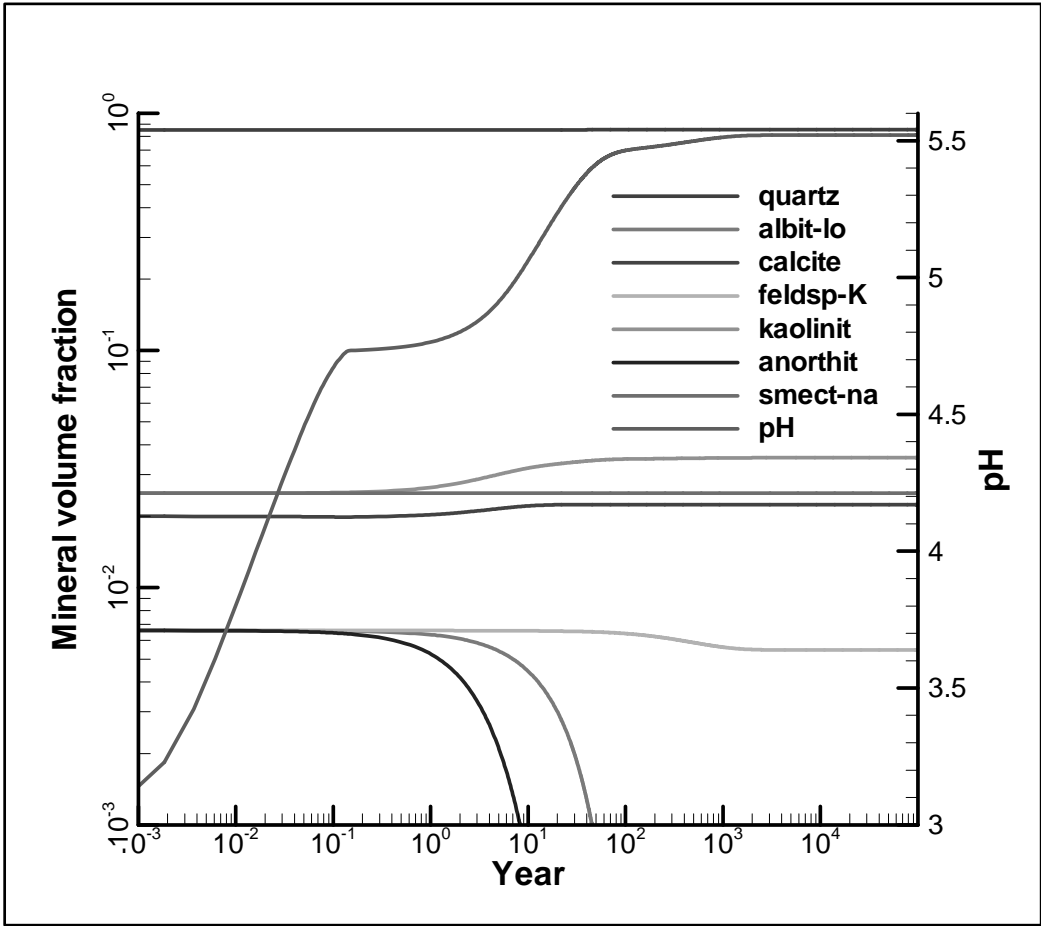


Figure 9: Changes in reservoir mineralogy as a result of reacting with a brine in equilibrium with CO_2 at 260 Bars. Porosity is not included in the calculation of mineral fraction.

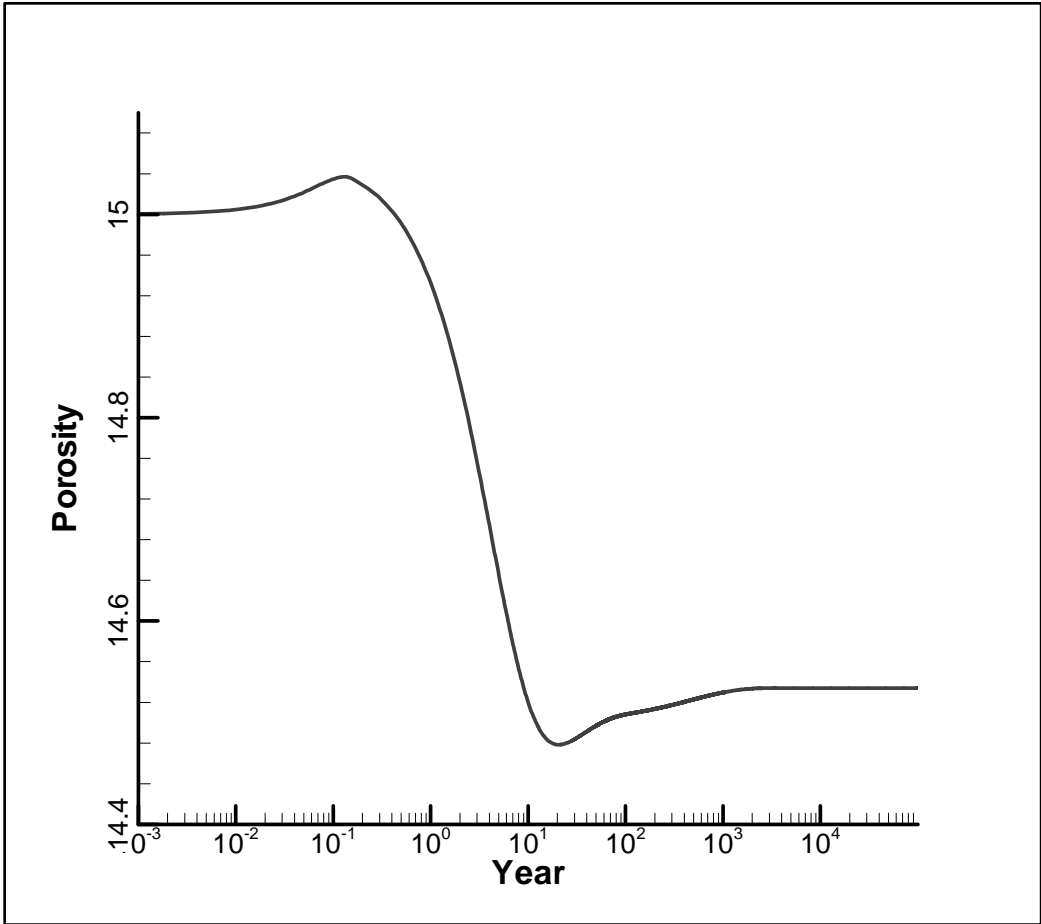


Figure 10: Change in reservoir porosity through reaction with CO₂ rich brine.

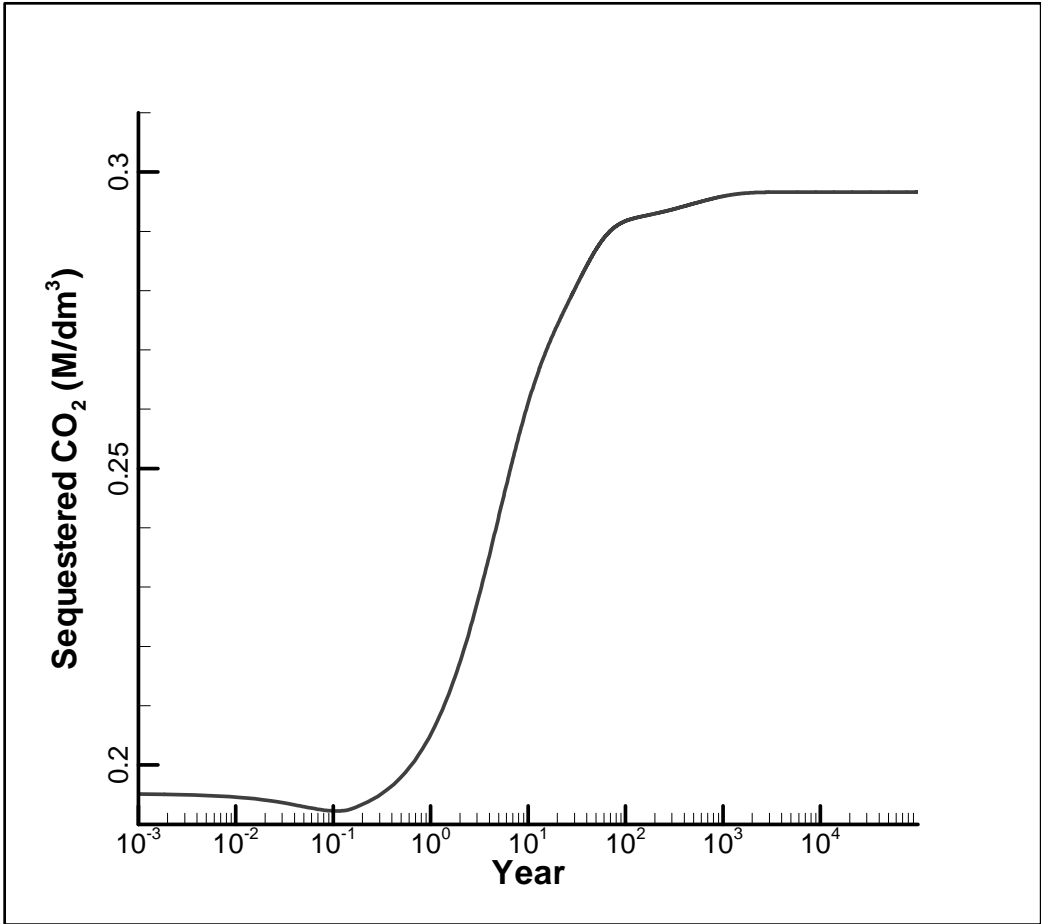


Figure 11: CO₂ sequestered as a mineral or dissolved in reservoir fluid.